

Matching Active Site and Substrate Structures for an RNA Editing Reaction

Subhash Pokharel,[‡] Prasanna Jayalath,[†] Olena Maydanovych,[‡] Rena A. Goodman,[†]
Selina C. Wang,[†] Dean J. Tantillo,[†] and Peter A. Beal^{*†}

Department of Chemistry, University of California, Davis, California 95616, and Department of Chemistry, University of Utah, 315 South 1400 East, Salt Lake City, Utah 84112-0850

Received April 27, 2009; E-mail: beal@chem.ucdavis.edu

Abstract: The RNA-editing adenosine deaminases (ADARs) catalyze deamination of adenosine to inosine in a double-stranded structure found in various RNA substrates, including mRNAs. Here we present recent efforts to define structure/activity relationships for the ADAR reaction. We describe the synthesis of new phosphoramidites for the incorporation of 7-substituted-8-aza-7-deazaadenosine derivatives into RNA. These reagents were used to introduce the analogues into mimics of the R/G-editing site found in the pre-mRNA for the human glutamate receptor B subunit (GluR B). Analysis of the kinetics of the ADAR2 reaction with analogue-containing RNAs indicated 8-aza-7-deazaadenosine is an excellent substrate for this enzyme with a deamination rate eight times greater than that for adenosine. However, replacing the C7 hydrogen in this analogue with bromine, iodine, or propargyl alcohol failed to increase the deamination rate further but rather decreased the rate. Modeling of nucleotide binding in the enzyme active site suggested amino acid residues that may be involved in nucleotide recognition. We carried out a functional screen of a library of ADAR2 mutants expressed in *S. cerevisiae* that varied the identity of these residues to identify active deaminases with altered active sites. One of these mutants (ADAR2 R455A) was able to substantially overcome the inhibitory effect of the bulky C7 substituents (–Br, –I, propargyl alcohol). These results advance our understanding of the importance of functional groups found in the edited nucleotide and the role of specific active site residues of ADAR2.

Introduction

Pathways for the regulation of gene expression that operate via modification of mRNA (or pre-mRNA) are recognized for their potential in the development of new therapeutics.¹ For instance, recent advances in the discovery of small molecules capable of modulating alternative splicing have led to the pharmacological control of disease-relevant pre-mRNAs.² In addition, antagonists of microRNA-programmed knockdown of specific messages are showing therapeutic potential for hypercholesterolemia and chronic hepatitis C infections.³ Adenosine to inosine RNA editing catalyzed by RNA-editing adenosine deaminase (ADAR) enzymes is another example of post-transcriptional regulation of gene expression. Thousands of human transcripts are targets for A to I RNA editing with the majority of these reactions occurring in untranslated regions for yet to be defined reasons.⁴ However, many examples are known of recoding that occurs when the editing event takes place within

an exon at a position in a codon that changes its meaning.^{5,6} These sites are often in mRNAs encoding proteins important for nervous system function such as glutamate receptors,⁷ serotonin receptors,⁸ and voltage gated ion channels.⁹ ADAR knockout animals often display developmental defects but also have defects in their nervous systems arising from the lack of these critical editing events.^{10–13} Importantly, a recent report describes a link between high levels of RNA editing in the pre-mRNA of the 2C subtype of the serotonin receptor and Prader-Willi syndrome, a congenital human disease with both developmental and behavioral symptoms.¹⁴ In addition, Gallo and co-workers have discovered a role for ADAR activity in controlling cell proliferation and migration in pediatric astrocytomas.¹⁵ Despite the clear importance of the A to I editing process in controlling gene expression and in human disease, no reasonably potent low molecular weight inhibitors are known for ADARs. Nor have any high-resolution structures of ADAR–substrate complexes been reported. Efforts in these areas will benefit from a more complete

[‡] University of Utah.

[†] University of California.

- (1) Cooper, T. A.; Wan, L.; Dreyfuss, G. *Cell* **2009**, *136*, 777–793.
- (2) Soret, J.; Bakkour, N.; Maire, S.; Durand, S. b.; Zekri, L.; Gabut, M.; Fic, W.; Divita, G.; Rivalle, C.; Dauzonne, D.; Nguyen, C. H.; Jeanteur, P.; Tazi, J. *Proc. Natl. Acad. Sci. U.S.A.* **2005**, *102*, 8764–8769.
- (3) Elmen, J.; Lindow, M.; Schutz, S.; Lawrence, M.; Petri, A.; Obad, S.; Lindholm, M.; Hedtjarn, M.; Hansen, H. F.; Berger, U.; Gullans, S.; Kearney, P.; Sarnow, P.; Straarup, E. M.; Kauppinen, S. *Nature* **2008**, *452*, 896–899.
- (4) Bhuiya, M. W.; Rittery, E. M.; Bernard A. Brown, I. In *RNA and DNA Editing*; Harold, C. S., Ed.; Wiley-Interscience: Hoboken, NJ, 2008; pp 340–368.

- (5) Jepson, J. E. C.; Reenan, R. A. *Biochim. Biophys. Acta, Gene Regul. Mech.* **2008**, *1779*, 459–470.
- (6) Li, J. B.; Levanon, E. Y.; Yoon, J.-K.; Aach, J.; Xie, B.; LeProust, E.; Zhang, K.; Gao, Y.; Church, G. M. *Science* **2009**, *324*, 1210–1213.
- (7) Higuchi, M.; Single, F. N.; Koehler, M.; Sommer, B.; Sprengel, R.; Seeburg, P. H. *Cell* **1993**, *75*, 1361–70.
- (8) Burns, C. M.; Chu, H.; Rueter, S. M.; Hutchinson, L. K.; Canton, H.; Sanders-Bush, E.; Emeson, R. B. *Nature* **1997**, *387*, 303–308.
- (9) Bhalla, T.; Rosenthal, J. J. C.; Holmgren, M.; Reenan, R. *Nat. Struct. Mol. Biol.* **2004**, *11*, 950–956.

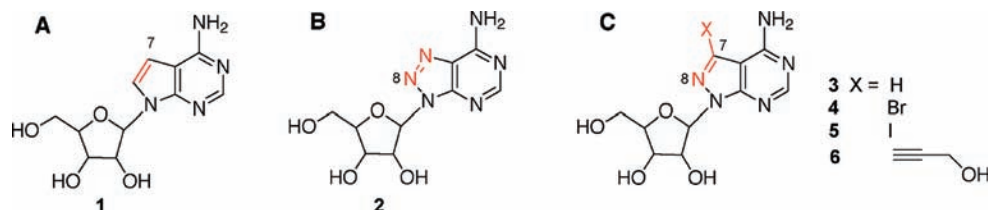


Figure 1. Nucleoside analogues introduced into ADAR2 substrate RNAs. (A) 7-deazaadenosine,¹⁷ (B) 8-azaadenosine,²³ (C) 8-aza-7-deazaadenosine and 7-substituted-8-aza-7-deazaadenosines (this work).

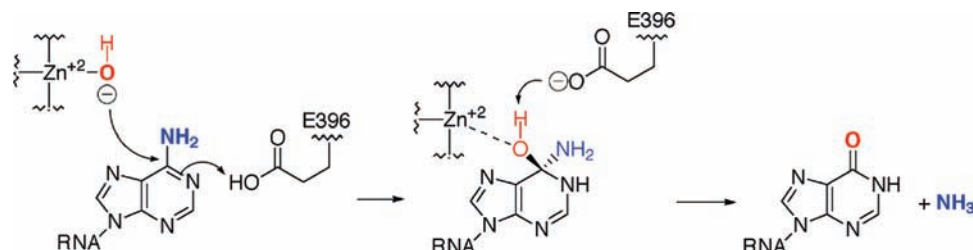


Figure 2. Proposed stepwise mechanism for adenosine deamination catalyzed by ADAR2.

understanding of the ADAR mechanism and its structure/activity relationships.

Biochemical studies and structures of ADAR fragments have shed some light on how these enzymes recognize substrates and catalyze adenosine deamination in RNA.^{16–32} In general, members of the ADAR family contain multiple RNA-binding motifs that bind double-stranded RNA substrates in addition to a zinc-containing catalytic domain where deamination occurs.^{28,33,34} Interestingly, the ADAR catalytic domain shares sequence similarity with cytidine deaminases (CDAs), enzymes that catalyze deamination of cytidine to uridine.^{35–37} Indeed, the crystal structure of the human ADAR2 deaminase domain revealed a CDA-like active site with structural variations near the periphery that are likely responsible for the adenosine specificity associated with ADARs.²⁸ However, the crystal structure of this domain lacks any ligand in the active site. Our understanding of adenosine recognition by ADARs relies on models based on this structure and that of CDAs bound to nucleoside inhibitors.^{28,38}

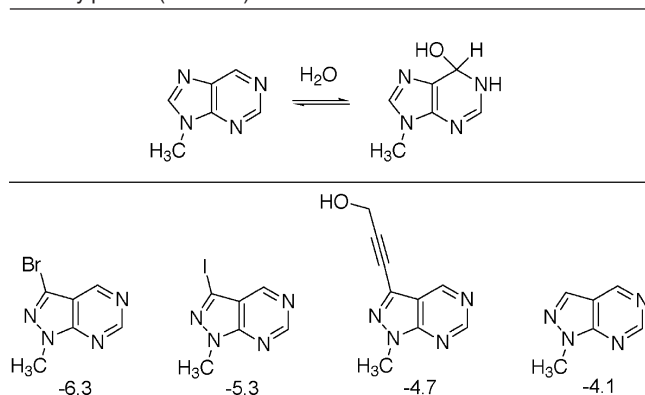
Our laboratory has used the reactivity of adenosine analogues in RNA as a means of probing substrate recognition in the ADAR reaction.^{17,23,25,32,39,40} For instance, we have shown that 7-deazaadenosine **1** in RNA is a good substrate for ADAR2, indicating that N7 can be removed with little to no effect on ADAR reactivity (Figure 1A).¹⁷ In contrast, introduction of nitrogen into adenosine at position 8 (8-azaadenosine **2**) substantially enhances ADAR reactivity (Figure 1B).²³ This observation led us to prepare RNA containing 8-azanebularine, which is capable of trapping ADAR2 in a high affinity complex, likely via the covalent hydrate.²⁵ Here we describe the effect of combining the 7-deaza- and the 8-aza modifications of adenosine (8-aza-7-deazaadenosine **3**) (Figure 1C). In addition, we describe new RNA editing substrates containing 7-substituted-8-aza-7-deazaadenosines **4–6** bearing different C7 groups and the role of active site structure in controlling ADAR2's reaction with these compounds. The results of these studies further define the importance of specific functional groups in the reactive nucleotide and their interaction with ADAR active site residues

and will lead to new approaches to targeting ADARs with nucleoside/oligonucleotide ligands.

Results

Our design of substrate analogues for ADAR2 is guided by the proposed reaction mechanism shown in Figure 2. ADARs deaminate adenosines within (or immediately adjacent to) a duplex secondary structure, so the enzyme must first extrude

- Higuchi, M.; Maas, S.; Single, F. N.; Hartner, J.; Rozov, A.; Burnashev, N.; Feldmeyer, D.; Sprengel, R.; Seeburg, P. H. *Nature* **2000**, *406*, 78–81.
- Palladino, M. J.; Keegan, L. P.; O'Connell, M. A.; Reenan, R. A. *Cell* **2000**, *102*, 437–449.
- Tonkin, L. A.; Saccomanno, L.; Morse, D. P.; Brodigan, T.; Krause, M.; Bass, B. L. *EMBO J.* **2002**, *21*, 6025–6035.
- Wang, Q.; Khillan, J.; Gadue, P.; Nishikura, K. *Science* **2000**, *290*, 1765–1768.
- Kishore, S.; Stamm, S. *Science* **2006**, *311*, 230–232.
- Cenci, C.; Barzotti, R.; Galeano, F.; Corbelli, S.; Rota, R.; Massimi, L.; Di Rocco, C.; O'Connell, M. A.; Gallo, A. *J. Biol. Chem.* **2008**, *283*, 7251–7260.
- Yi-Brunozzi, H. Y.; Easterwood, L. M.; Kamilar, G. M.; Beal, P. A. *Nucleic Acids Res.* **1999**, *27*, 2912–2917.
- Easterwood, L. M.; Veliz, E. A.; Beal, P. A. *J. Am. Chem. Soc.* **2000**, *122*, 11537–11538.
- Stephens, O. M.; Yi-Brunozzi, H. Y.; Beal, P. A. *Biochemistry* **2000**, *39*, 12243–12251.
- Veliz, E. A.; Stephens, O. M.; Beal, P. A. *Org. Lett.* **2001**, *3*, 2969–2972.
- Yi-Brunozzi, H. Y.; Stephens, O. M.; Beal, P. A. *J. Biol. Chem.* **2001**, *276*, 37827–37833.
- Cho, D.-S. C.; Yang, W.; Lee, J. T.; Shiekhatter, R.; Murray, J. M.; Nishikura, K. *J. Biol. Chem.* **2003**, *278*, 17093–17102.
- Gallo, A.; Keegan, L. P.; Ring, G. M.; O'Connell, M. A. *EMBO J.* **2003**, *22*, 3421–3430.
- Veliz, E. A.; Easterwood, L. M.; Beal, P. A. *J. Am. Chem. Soc.* **2003**, *125*, 10867–10876.
- Dawson, T. R.; Sansam, C. L.; Emeson, R. B. *J. Biol. Chem.* **2004**, *279*, 4941–4951.
- Haudenschild, B. L.; Maydanovych, O.; Veliz, E. A.; Macbeth, M. R.; Bass, B. L.; Beal, P. A. *J. Am. Chem. Soc.* **2004**, *126*, 11213–11219.
- Macbeth, M. R.; Lingam, A. T.; Bass, B. L. *RNA* **2004**, *10*, 1563–1571.
- Stephens, O. M.; Haudenschild, B. L.; Beal, P. A. *Chem. Biol.* **2004**, *11*, 1239–1250.
- Macbeth, M. R.; Schubert, H. L.; VanDemark, A. P.; Lingam, A. T.; Hill, C. P.; Bass, B. L. *Science* **2005**, *309*, 1534–1539.
- Maydanovych, O.; Beal, P. A. *Chem. Rev.* **2006**, *106*, 3397–3411.
- Pokharel, S.; Beal, P. A. *ACS Chem. Biol.* **2006**, *1*, 761–765.

Table 1. Computed Hydration Free Energy Relative to 9-Methylpurine (kcal/mol)

the nucleotide to be edited from the duplex and into the zinc-containing active site (i.e., an initial base flipping step). Then in an S_NAr -type reaction, attack of a zinc-bound hydroxide ion and N1 protonation generates the covalent hydrate of the adenine ring (i.e., the Messenheimer intermediate). Proton transfer from hydroxyl to the leaving amine is followed by departure of ammonia and formation of the inosine product. Recent kinetic isotope studies with the related tRNA modifying enzyme Tada are consistent with this proposal.⁴¹

Considering this mechanism, one might expect the propensity to form a covalent hydrate by the addition of water across the C6–N1 double bond for various purine analogues to be a good predictor of the C6 deamination rate for related substrates. Indeed, the hydrate of 8-azapurine is significantly more stable (based on computed hydration free energies) than that of purine, while 8-azaadenosine in RNA is deaminated much more rapidly by ADAR2 than is adenosine.^{23,42} This correlation between the stability of covalent hydrates and rate of deamination for related amino-substituted compounds has been observed for other heterocycles.^{42–47} In an attempt to predict the ADAR reactivity of 7-substituted-8-aza-7-deazaadenosines, we computed covalent hydration free energies using density functional theory (DFT) for a group of 8-aza-7-deazapurine analogues bearing a 9-methyl group (see Experimental Section for computational details) (Table 1). These compounds included 7-bromo and 7-iodo

analogues, allowing for an assessment of the effect of different halogens. In addition, the 7-propargyl alcohol derivative was analyzed. This analogue was chosen as an example of a derivative with a more sterically demanding C7 substituent linked via a carbon–carbon bond. Also, since a variety of alkyne-containing substituents can be introduced via Sonogashira couplings with a C7 halo precursor, it was important to evaluate the effect of a simple C7-alkynyl modification to guide the design of additional new analogues bearing this linkage.

The DFT calculations indicate that an 8-aza-7-deazapurine is more readily hydrated than a simple purine. Furthermore, the calculations suggest that the hydrates of the 7-substituted-8-aza-7-deazapurines are more stable than that of the unsubstituted analogue (Table 1) with the hydrate of the 7-bromo compound the most stable of this group. Therefore, if only the intrinsic reactivity of the base is considered, one would expect the corresponding 8-aza-7-deazaadenosines to be competent substrates for ADARs with the 7-bromo analogue reacting the fastest. More difficult to predict is how these modifications might affect the base-flipping step of the ADAR reaction. Furthermore, this analysis does not consider steric effects and how they may affect the fit of the nucleoside analogue within the enzyme active site.

To test the reactivity of these analogues in an ADAR reaction, we prepared phosphoramidites necessary to introduce them into duplex RNA substrates for human ADAR2. Nucleosides **3–5** were known compounds prior to our work (Figure 1). The propargyl alcohol derivative was prepared from 7-iodo-8-aza-7-deazaadenosine **7** via a Sonogashira coupling to give **8** in good yield (Scheme 1). Silyl protection of the propargyl alcohol followed by removal of the ribose protecting groups gave nucleoside **10**.

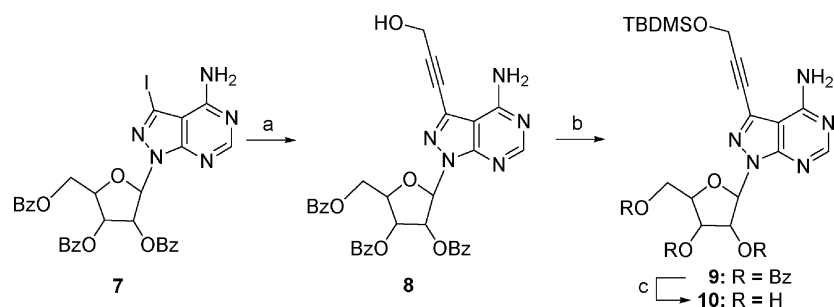
Nucleosides **3–5** and **10** were each protected at the C6 amine as the dimethylacetamide (Scheme 2). Dimethoxytrityl protection of the 5'-hydroxyls along with 2'-*O*-TBDMS protection and phosphorylation gave phosphoramidites **23–26** necessary for generation of modified RNA (Scheme 2).

These phosphoramidites were used to prepare oligoribonucleotides corresponding to a sequence found near the R/G editing site in human GluR B pre-mRNA (Table 2). We have used this duplex substrate in the past for evaluating the effect of adenosine modifications on the ADAR2 reaction.^{16,18,23} Each of the new phosphoramidites coupled efficiently during automated RNA synthesis and survived RNA deprotection conditions unaltered as indicated by ESI-MS of the purified oligonucleotide products (see Supporting Information).

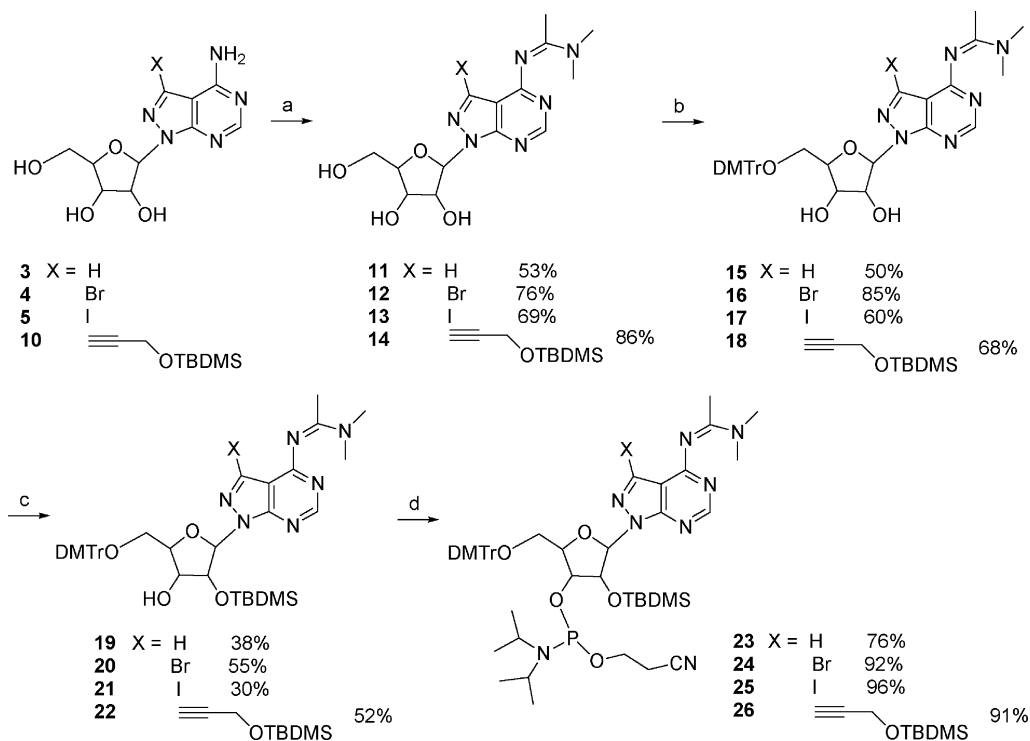
The effect each modification had on the ADAR2 deamination rate was evaluated under single turnover conditions at the saturating concentration of the enzyme. These conditions were chosen, since kinetic studies with ADAR2, where [substrate] \gg [enzyme], are complicated by long reaction times for this RNA substrate.¹⁸ In addition, ADAR2 substrates that differ only in structure at the reactive adenosine typically vary little in measured binding affinity (K_d) due to the dominant role played by the duplex RNA-binding domain in determining the affinity for substrate (see below and Figure S.1).^{18,23} However, large differences can be observed in the rate constant for deamination measured under single turnover conditions at saturating enzyme concentration for various adenosine analogues in this RNA.^{16,17,23}

We found that 8-aza-7-deazaadenosine (**3**) at the R/G site was deaminated to product by ADAR2 with a rate of $0.53 \pm 0.03 \text{ min}^{-1}$ (Table 2). This rate is nearly eight times faster than that for adenosine at the same site in this substrate.^{16,23} The

- (31) Stefl, R.; Xu, M.; Skrisovska, L.; Emeson, R. B.; Allain, F. H.-T. *Structure* **2006**, *14*, 345–355.
- (32) Maydanovych, O.; Easterwood, L. M.; Cui, T.; Veliz, E. A.; Pokharel, S.; Beal, P. A. *Methods Enzymol.* **2007**, *424*, 369–86.
- (33) Bass, B. L.; Weintraub, H. *Cell* **1987**, *48*, 607–13.
- (34) Doyle, M.; Jantsch, M. F. *J. Cell Biol.* **2003**, *161*, 309–319.
- (35) Melcher, T.; Maas, S.; Herb, A.; Sprengel, R.; Seeburg, P. H.; Higuchi, M. *Nature* **1996**, *379*, 460–4.
- (36) Kim, U.; Wang, Y.; Sanford, T.; Zeng, Y.; Nishikura, K. *Proc. Natl. Acad. Sci. U.S.A.* **1994**, *91*, 11457–61.
- (37) Carter, C. W., Jr. *Biochimie* **1995**, *77*, 92–8.
- (38) Betts, L.; Xiang, S.; Short, S. A.; Wolfenden, R.; Carter, C. W., Jr. *J. Mol. Biol.* **1994**, *235*, 635–56.
- (39) Maydanovych, O.; Beal, P. A. *Org. Lett.* **2006**, *8*, 3753–3756.
- (40) Jayalath, P.; Pokharel, S.; Veliz, E.; Beal, P. A. *Nucleosides, Nucleotides, Nucleic Acids* **2009**, *28*, 78–88.
- (41) Luo, M.; Schramm, V. L. *J. Am. Chem. Soc.* **2008**, *130*, 2649–2655.
- (42) Erion, M. D.; Reddy, M. R. *J. Am. Chem. Soc.* **1998**, *120*, 3295–3304.
- (43) Evans, B.; Wolfenden, R. *Biochemistry* **1973**, *12*, 392–398.
- (44) Agarwal, R. P.; Sagar, S. M.; Parks, R. E., Jr. *Biochem. Pharmacol.* **1975**, *24*, 693–701.
- (45) Albert, A. *Adv. Heterocycl. Chem.* **1976**, *20*, 117–43.
- (46) Shewach, D. S.; Krawczyk, S. H.; Acevedo, O. L.; Townsend, L. B. *Biochem. Pharmacol.* **1992**, *44*, 1697–700.
- (47) Hernandez, S.; Ford, H.; Marquez, V. E. *Bioorg. Med. Chem.* **2002**, *10*, 2723–2730.

Scheme 1^a

^a Conditions: (a) Pd(PPh₃)₄, CuI, Et₃N, CHCCH₂OH, DMF, 86%; (b) TBDMSCl, Et₃N, DCM, 79%; (c) NaOMe/MeOH 70%.

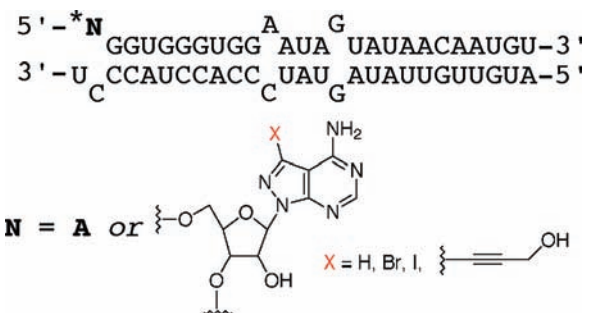
Scheme 2^a

^a Conditions: (a) CH₃C(OCH₃)₂N(CH₃)₂, CH₃OH; (b) DMTCl, pyridine, AgNO₃, THF; (c) TBDMSCl, AgNO₃, Et₃N, THF; (d) CIP(OCH₂CH₂CN)(N(*i*Pr)₂), DIPEA, THF.

large rate acceleration observed for **3** is similar to that found for 8-azaadenosine (**2**), underscoring the importance of the 8-aza modification.²³ Also, this observation confirmed the 7-deaza modification has minimal effect on the ADAR2 reaction. Interestingly, under the same reaction conditions, 7-bromo-8-aza-7-deazaadenosine (**4**) was a slower substrate than **3**, with a rate of deamination similar to that for adenosine (0.08 min⁻¹) (Table 2). In addition, the 7-iodo compound (**5**) and 7-propargyl alcohol compound (**6**) each were converted to product substantially more slowly than **3** (88-fold and 176-fold, respectively) in this RNA. Indeed, the rate of deamination for each of these two analogues was >10-fold lower than that observed for adenosine (Table 2). As expected from our previous studies, these effects are not due to differences in binding since all four RNA substrates (where X = H, Br, I, or propargyl alcohol (Table 2)) are completely bound at this ADAR2 concentration (Figure S.1).²³

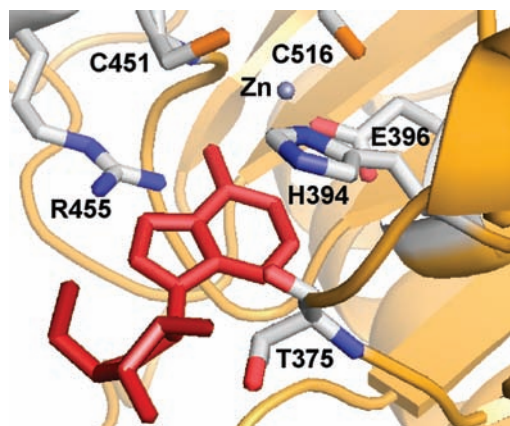
The observation that RNAs modified with 7-substituted 8-aza-7-deazaadenosines **4–6** were slower substrates than 8-aza-7-deazaadenosine **3** was somewhat surprising, since these substitu-

ents were expected to accelerate the rate of deamination based on their intrinsic propensities to hydrate (see above). However, analysis of the crystal structure of the catalytic domain of ADAR2 with AMP modeled into the active site suggested a possible clash between a bulky substituent at the purine 7-position and the side chain of R455 (Figure 3).²⁸ We hypothesized that such an unfavorable interaction within the enzyme/substrate complex may cause a poor fit within the active site and contribute to the lower than expected rate of deamination for the 7-substituted compounds. To test this idea, we used a screen developed previously in our laboratory to identify functional mutants of ADAR2 with altered active site residues.³⁰ The screen relies on the ability of active ADAR2 mutants to deaminate within a stop codon in frame with the coding sequence for the reporter enzyme α -galactosidase while both enzyme and substrate RNA are expressed in the yeast *S. cerevisiae*. The ADAR reaction converts the stop codon to one for tryptophan, and expression of the reporter is observed as colored yeast colonies. For this study, two amino acid positions were chosen for randomization (375 and 455 in the human

Table 2. Single Turnover Rate Constants for Reaction of ADAR2 with RNAs Bearing 7-Substituted-8-aza-7-deazaadenosine Analogues^a


enzyme	substrate (N)	k_{obs} , min ^{-1b}	k_{rel}^c
ADAR2	A	0.07 ± 0.03	1
	X = H	0.53 ± 0.03	7.6
	X = Br	0.08 ± 0.01	1.1
	X = I	0.006 ± 0.001	0.09
	X = CCCH ₂ OH	0.003 ± 0.0003	0.04

^a Reactions were carried out with 250 nM enzyme, 25 nM RNA substrate. ^b Data were fitted to the equation: $[P]_t = \alpha[1 - \exp(-k_{\text{obs}} \cdot t)]$. ^c $k_{\text{rel}} = k_{\text{obs}}$ for analogue/ k_{obs} for adenosine.

**Figure 3.** ADAR2 active site. Active site residue positions for human ADAR2 as determined by X-ray crystallography for the catalytic domain.²⁸ AMP (red) has been modeled into this active site based on structures of the related CDAs bound to inhibitors.³⁸

ADAR2 sequence) that are not conserved in the ADAR family but are in locations near the entrance to the zinc-containing active site and may be involved in nucleotide recognition (Figure 3).²⁸ If functional mutants of ADAR2 could be discovered with different active site recognition properties, nucleoside analogues, such as the 7-substituted 8-aza-7-deazaadenosines described here, may function as substrates (or inhibitors).^{48–52}

Saturation mutagenesis was carried out at the codons for residues 375 and 455 of human ADAR2. The resulting plasmid library was then used to screen for mutants active for RNA editing in our screen. A total of 22 active clones were sequenced and 14 unique DNA sequences were identified corresponding

Table 3. Results of Screening ADAR2 T375X,R455X Library

codon(s)	no. of clones	Amino acids (375, 455)
AGT, GCT	1	Ser, Ala
AGT, AGC	2	Ser, Ser
ACC, CGT	2	Thr, Arg
TCG, GGC	2	Ser, Gly
AGT, ACA	1	Ser, Thr
AGT, AGA	2	Ser, Arg
GGG, TCG	3	Gly, Ser
TGC, AGA	2	Cys, Arg
TCA, TCA	1	Ser, Ser
AGT, AGT	1	Ser, Ser
AGT, AGA	2	Ser, Arg
AGC, GCG	1	Ser, Ala
TCC, GGT	1	Ser, Gly
ACA, GCA	1	Thr, Ala

Table 4. Single Turnover Rate Constants for Reaction of ADAR2(R455A) with RNAs Bearing 7-Substituted-8-aza-7-deazaadenosine Analogues^a

enzyme	substrate (N) ^b	k_{obs} , min ^{-1c}	k_{rel}^d
ADAR2(R455A)	A	0.037 ± 0.002	1
	X = H	0.13 ± 0.004	3.5
	X = Br	0.22 ± 0.01	5.9
	X = I	0.05 ± 0.01	1.4
	X = CCCH ₂ OH	0.05 ± 0.004	1.4

^a Reactions were carried out with 250 nM enzyme, 25 nM RNA substrate. ^b Substrate RNA as seen in Table 2. ^c Data were fitted to the equation: $[P]_t = \alpha[1 - \exp(-k_{\text{obs}} \cdot t)]$. ^d $k_{\text{rel}} = k_{\text{obs}}$ for analogue/ k_{obs} for adenosine.

to 9 different protein sequences. A summary of the results of the screen is found in Table 3. Interestingly, a large fraction (8/9) of mutants identified had small hydrogen bond donors (threonine, serine, or cysteine) at position 375. This is consistent with the proposed role of this residue in a hydrogen-bonding interaction with the 2' hydroxyl of the reactive nucleotide.³⁰ Importantly, several small residues were found in the active pool at position 455 (alanine, serine, threonine, and glycine). Thus, a critical interaction between the guanidinium group of R455 and the purine ring of the reactive nucleotide seems unlikely. Furthermore, these smaller active site residues may allow ADAR2 to process more sterically demanding substrates. Along these lines, we chose to study further the R455A mutant. This protein was overexpressed and purified as previously described.²⁶ RNA substrates containing adenosine and the 7-deaza-8-azaadenosines **3–6** were then subjected to the reaction of the ADAR2 R455A mutant. Importantly, this mutant is nearly as active as wild type ADAR2 with adenosine at the R/G site, exhibiting rate constants within a factor of 2 for the two proteins (Tables 2, 4).

However, the reactivity profile for the different analogues is markedly different with the R455A mutant compared to the wild type enzyme. With this enzyme, all the 8-aza-7-deazaadenosine analogues tested were at least as reactive as, if not superior to, adenosine in this substrate context. RNA containing 7-bromo-8-aza-7-deazaadenosine **4** was the best substrate, with a rate nearly six times higher than that for adenosine (Table 4). 8-Aza-7-deazaadenosine also reacts faster than adenosine, but only by 3.5-fold (compared to 8-fold higher for wild type ADAR2). RNAs containing both the 7-iodo compound **5** and 7-propargyl alcohol derivative **6** were good substrates for the mutant with rates slightly higher than that for adenosine. Importantly, each of the analogues with “bulky” substituents at C7 (**4–6**) had faster rates with the R455A mutant than with the wild type

- (48) Clemons, P. A.; Gladstone, B. G.; Seth, A.; Chao, E. D.; Foley, M. A.; Schreiber, S. L. *Chem. Biol.* **2002**, *9*, 49–61.
 (49) Kraybill, B. C.; Elkin, L. L.; Blethrow, J. D.; Morgan, D. O.; Shokat, K. M. *J. Am. Chem. Soc.* **2002**, *124*, 12118–12128.
 (50) Shah, K.; Shokat, K. M. *Chem. Biol.* **2002**, *9*, 35–47.
 (51) Belshaw, P. J.; Schreiber, S. L. *J. Am. Chem. Soc.* **1997**, *119*, 1805–1806.
 (52) Lin, Q.; Jiang, F.; Schultz, P. G.; Gray, N. S. *J. Am. Chem. Soc.* **2001**, *123*, 11608–11613.

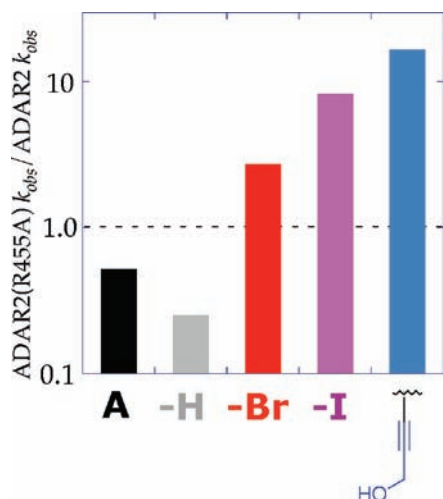


Figure 4. R455A mutation of ADAR2 accelerates the deamination for analogues with bulky substituents at C7 of 8-aza-7-deazaadenosine.

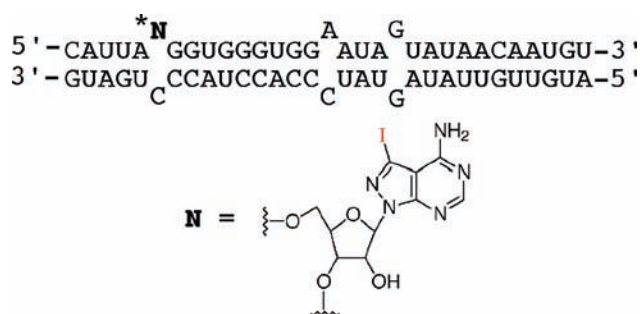


Figure 5. 31-mer R/G site RNA substrate used to assay wild type ADAR2 and ADAR2(R455A) editing activity. GluR-B R/G site indicated by N is substituted with modified nucleotide analogue.

enzyme (R455A k_{obs} /ADAR2 k_{obs} > 1.0), whereas adenosine and 8-aza-7-deazadenosine reacted faster with wild type ADAR2 (R455A k_{obs} /ADAR2 k_{obs} < 1.0) (Figure 4).

The substrate RNA used for the studies described above bears the reactive nucleotide at the 5' end of the RNA duplex (Table 2). We use this test substrate design because it facilitates data acquisition since simple end labeling of the top strand tags the reactive nucleotide with a radioactive phosphate, necessary for our TLC-based assay. However, editing site adenosines in natural substrates are most often flanked on both sides by a duplex structure. To determine the effect of a flanking duplex structure on the reactivity of a 7-substituted-8-aza-7-deazaadenosine, we prepared a substrate using end labeling and splint ligation as previously described by us to add RNA structure 5' to a labeled editing site (Figure 5).¹⁸ As expected, this change in RNA structure accelerates adenosine deamination for both wild type ADAR2 and the R455A mutant (wild type ADAR2 rate = 0.8 min⁻¹, R455A rate = 0.4 min⁻¹) (data not shown). However, with the 7-iodo derivative **5** at the editing site, the wild type ADAR2 rate decreased 3-fold (to $2 \pm 0.2 \times 10^{-3}$ min⁻¹) and the R455A rate increased slightly (to 0.08 ± 0.002 min⁻¹) in comparison to the shorter substrate. Thus, the reactivity of the 7-iodo compound is suppressed even further

in this substrate relative to adenosine, but it reacts 40 times faster with the R455A mutant than it does with wild type ADAR2.

Discussion

Tight binding nucleoside analogues are valuable in ADAR structural studies and could function as inhibitors.^{53,54} We had previously shown that 8-azapurines are well suited for binding the ADAR2 active site.²⁵ This is most likely due to the fact that 8-azapurine is more susceptible than purine to covalent hydration, a key step in the deamination mechanism (Figure 2).⁴² Thus, 8-azapurine analogues were promising as new ligands for ADARs. However, derivatives with substituents at C2 or C6 bound poorly to ADAR2.^{23,39} For these reasons, we were interested in the ADAR reactivity of 8-aza-7-deazaadenosine and 7-substituted derivatives. If these were found to be good ADAR substrates, one could imagine developing new ligands with substituents at C7 capable of stabilizing contacts with the ADAR active site (or that of a mutant). Furthermore, these compounds could be used to test the existing substrate recognition model.

Reactivity of Analogues and Mutants Support Nucleotide Binding Model for ADAR2 Active Site. The model for nucleotide binding in the ADAR2 active site suggests a close approach between the side chain of R455 and adenine N7 (Figure 3). Interestingly, the nucleoside-modifying enzyme adenosine deaminase (ADA) binds its substrate via hydrogen bonds to each of the purine nitrogens, including N7.⁵⁵ An aspartic acid in the ADA active site (D296 in mouse ADA) hydrogen bonds to N7, and this residue is critical for activity (0.001% of wild type k_{cat}/K_m for the D296A mutation). In addition, removal of N7 from the substrate is highly inhibitory to the ADA reaction, and 7-substituted 7-deaza compounds are poor ADA substrates.^{56,57} In contrast, an important, direct interaction between the R455 side chain of ADAR2 and substrate N7 is unlikely, since 7-deazaadenosine and 8-aza-7-deazaadenosine in RNA are both good substrates¹⁷ (Tables 2, 4) and mutants of ADAR2 that vary the position 455 residue have near wild type activity, including R455A (Table 3). One can understand the difference in importance of the interaction between the enzyme and N7 of the adenine for the different types of adenosine deaminases when one considers that ADARs bind their substrates tightly via their RNA-binding domains and are not as dependent on specific interactions to the reacting base to hold the substrate in the active site (as is the case for the nucleoside processing enzyme ADA). Indeed, dissociation constants for RNA binding to the isolated RNA-binding domain of ADAR2 are similar in magnitude to those for the full-length enzyme.^{20,27}

Nevertheless, the R455A mutation in ADAR2 clearly compensates for the poor reactivity of the wild type enzyme with analogues that project sterically demanding substituents from the C7 position of 8-aza-7-deazaadenosine (Br, I, propargyl alcohol) (Figure 4). Thus, we conclude that substrate N7 and the R455 side chain are in proximity at some point during the reaction but their interaction is not necessary for editing. This observation has important implications for future design of nucleotide-based ligands for ADARs. Since both the C7 position of a 7-deazapurine substrate and the R455 residue of ADAR2

(53) Verdine, G. L.; Norman, D. P. G. *Annu. Rev. Biochem.* **2003**, *72*, 337–366.

(54) Jiang, Y. L.; Krosky, D. J.; Seiple, L.; Stivers, J. T. *J. Am. Chem. Soc.* **2005**, *127*, 17412–17420.

(55) Wilson, D. K.; Rudolph, F. B.; Quijcho, F. A. *Science* **1991**, *252*, 1278–84.

(56) Frederiksen, S. *Arch. Biochem. Biophys.* **1966**, *113*, 383–388.

(57) Seela, F.; Xu, K. *Org. Biomol. Chem.* **2007**, *5*, 3034–3045.

can be altered in ways that maintain a productive interaction between enzyme and substrate, these positions are good choices for engineering in new interactions, such as salt bridges or covalent cross-links. Stabilized complexes of this type have aided structural studies of other protein–nucleic acid interactions, and these efforts are currently underway in our laboratory.^{40,53} Furthermore, sequence alignment of human ADAR2 and ADAR1 indicate that ADAR1 has an alanine residue (A970) at the position corresponding to R455 in ADAR2.³⁶ Therefore, it is possible that 7-substituted 8-aza-7-deazaadenosine derivatives described here will be good substrates for wild type ADAR1, although this remains to be tested and will require development of a suitable in vitro substrate for ADAR1. If so, 7-substituted 8-aza-7-deazapurine analogues may be capable of differentiating ADAR1 from ADAR2.

Are C7 Analogues Difficult to Flip? Within the group of analogues with bulky C7 substituents, our DFT calculations on the stabilities of covalent hydrates were useful in predicting the relative reactivity of the substrate analogues (Br > I > CCCH₂OH) (Tables 1, 2, and 4). However, in contrast with the predicted result, all three of these were less reactive than 8-aza-7-deazaadenosine with wild type ADAR2. The increase in rate realized when introducing the R455A mutation explains some of this lower than expected reactivity as arising from a steric clash. However, even for the R455A mutant, the 7-iodo and 7-propargyl alcohol compounds were less reactive than 8-aza-7-deazaadenosine (Table 4). This inhibitory effect could arise for several reasons. For instance, base modification can alter the preferred sugar pucker in nucleosides, which has been shown to be a factor in controlling rates of enzyme-catalyzed nucleoside deamination.^{58–63} It is also true that halogens and alkynes at the 7-position of 7-deazapurines stabilize nucleic acid duplexes.^{64,65} Since the edited nucleotide must flip out of the duplex and into the ADAR active site, stabilization of a base-stacked conformation could inhibit this step and slow the reaction.^{18,20} Results with extended duplex substrates are consistent with this latter hypothesis (Figure 5). The rate of ADAR2-catalyzed adenosine deamination is higher when this nucleotide is flanked by a duplex on both sides, yet the 7-iodo analogue reacts more slowly in this context compared to its reactivity at the duplex end. It stands to reason that the reactive nucleotide would be less conformationally flexible within the extended duplex and the barrier for nucleotide flipping would be higher. Rates of flipping for the 7-iodo analogue will be needed to confirm that this step is the reason for the low reactivity observed. Once this is established, the 7-substituted analogues could be used to probe the role of base flipping in the various ADAR substrates where

the editing sites reside in duplexes with a varying flanking sequence, in internal loops, or at duplex sites with A•C or A•U pairs.

Experimental Section

General Synthetic Procedures. Glassware for all reactions was flame-dried or oven-dried at 175 °C overnight and cooled in a desiccator prior to use. Reactions were carried out under an atmosphere of dry nitrogen when anhydrous conditions were necessary. All reagents were purchased from commercial sources (Sigma/Aldrich or Fischer Scientific) and were used without further purification unless otherwise stated. Tetrahydrofuran was either distilled from sodium metal and benzophenone or passed through a column of activated aluminum.⁶⁶ TLC analysis of reaction mixtures was performed on Merck silica gel 60 F₂₅₄ precoated TLC plates. Short and long wave visualization was performed with a Mineralight multiband ultraviolet lamp at 254 and 365 nm, respectively. Flash column chromatography was performed on Mallinckrodt Baker silica gel 150 (60–200 mesh). ¹H, ¹³C, and ³¹P nuclear magnetic resonance spectra were recorded with Varian VNMRs 600, Varian Mercury 300 spectrometers and referenced to CDCl₃ unless otherwise noted. The abbreviations such as s, t, m, brs, dd, and d stand for singlet, triplet, multiplet, broad singlet, doublet of doublets, and doublet. High-resolution mass spectra were obtained at the Department of Chemistry, University of Utah or at the University of California, Davis and the University of California, San Diego Mass spectrometry facility.

4-Amino-3-(3''-hydroxy-1''-propynyl)-1-(2',3',5'-tri-*O*-benzoyl- β -D-ribofuranosyl)-1*H*-pyrazolo[3,4-*d*]pyrimidine (8). A suspension of **7** (518 mg, 0.734 mmol), Pd(PPh₃)₄ (104 mg, 0.09 mmol), and CuI (47.5 mg, 0.25 mmol) in anhydrous DMF (3 mL) was treated with propargyl alcohol (290 μ L, 3.67 mmol) followed by anhydrous triethylamine (81 μ L, 0.734 mmol). The mixture was stirred under Ar at room temperature. After the reaction was complete (TLC), the solvent was removed in vacuo, and the residue was chromatographed on a flash silica gel column, eluting with CH₂Cl₂–CH₃OH (95:5) to give **8** (398 mg, 86%) as a white form. ¹H NMR (CDCl₃, 600 MHz): δ (ppm) 8.31 (s, 1H), 8.08–7.93 (m, 5H), 7.55–7.33 (m, 10H), 6.80 (d, *J* = 3.0 Hz, 1H), 6.38 (dd, *J* = 3.0, 5.4 Hz, 1H), 6.30 (dd, *J* = 6.0, 6.6 Hz, 1H), 4.85 (dd, *J* = 1.8, 4.2 Hz, 1H), 4.76 (dd, *J* = 3.6, 12 Hz, 1H), 4.64 (dd, *J* = 4.8, 12 Hz, 1H), 4.55 (s, 2H). ¹³C NMR (CDCl₃, 150 MHz): δ (ppm) 166.6, 165.6, 165.5, 157.8, 157.1, 154.6, 133.9, 133.8, 133.3, 130.2, 130.1, 130.0, 129.8, 129.0, 128.9, 128.8, 128.7, 128.6, 128.5, 94.1, 87.2, 80.3, 77.1, 74.9, 72.1, 64.2, 51.4. ESIHRMS: calcd for C₃₄H₂₅N₅O₈ (M + H)⁺ 634.1938, obsd 634.1930.

4-Amino-3-(3''-*O*-*tert*-butyldimethylsilyloxypropyne)-1-(2',3',5'-tri-*O*-benzoyl- β -D-ribofuranosyl)-1*H*-pyrazolo[3,4-*d*]pyrimidine (9). To a suspension of **8** (324 mg, 0.51 mmol) and DMAP (50 mg) in CH₂Cl₂ (6 mL) was added TBDMSCl (116 mg, 0.77 mmol) followed by anhydrous triethylamine (0.11 mL, 1.0 mmol). The mixture was stirred under Ar at room temperature for 12 h and purified by flash silica gel column chromatography with CH₂Cl₂–CH₃OH (99:1) to give **9** as a white foam (304 mg, 79%). ¹H NMR (CDCl₃, 600 MHz): δ (ppm) 8.18 (s, 1H), 7.29–7.91 (m, 2H), 7.81–7.76 (m, 4H), 7.39–7.33 (m, 3H), 7.24–7.16 (m, 6H), 6.64 (d, *J* = 3.0 Hz, 1H), 6.20 (dd, *J* = 3.6, 5.4 Hz, 1H), 6.13 (t, *J* = 6.6 Hz, 1H), 5.91 (brs, 2H), 4.66 (dd, *J* = 4.8, 10.8 Hz, 1H), 4.57 (dd, *J* = 4.2, 12.0 Hz, 1H), 4.46 (dd, *J* = 4.8, 12.0 Hz, 1H), 4.44 (s, 2H), 0.77 (s, 9H), 0.01 (s, 6H). ¹³C NMR (CDCl₃, 150 MHz): δ (ppm) 166.4, 165.4, 165.2, 157.9, 157.3, 154.7, 133.7, 133.6, 133.5, 132.3, 130.1, 130.9, 129.9, 129.8, 129.0, 128.9, 128.6, 128.5, 128.50, 94.4, 87.2, 80.3, 76.6, 74.7, 72.0, 64.1, 52.3, 26.0, 25.9, 18.4, –5.02, –5.03. ESIHRMS: calcd for C₄₀H₄₂N₅O₈Si (M + H)⁺ 748.2803, obsd 748.2794.

- (58) Luyten, I.; Thibaudeau, C.; Chattopadhyaya, J. *J. Org. Chem.* **1997**, *62*, 8800–8808.
 (59) Jeong, L. S.; Buenger, G.; McCormack, J. J.; Cooney, D. A.; Hao, Z.; Marquez, V. E. *J. Med. Chem.* **1998**, *41*, 2572–2578.
 (60) Marquez, V. E.; Russ, P.; Alonso, R.; Siddiqui, M. A.; Hernandez, S.; George, C.; Nicklaus, M. C.; Dai, F.; Ford, H., Jr. *Helv. Chim. Acta* **1999**, *82*, 2119–2129.
 (61) Ford, H., Jr.; Dai, F.; Mu, L.; Siddiqui, M. A.; Nicklaus, M. C.; Anderson, L.; Marquez, V. E.; Barchi, J. J. *Biochemistry* **2000**, *39*, 2581–2592.
 (62) Seela, F.; Zulauf, M.; Debelak, H. *Helv. Chim. Acta* **2000**, *83*, 1437–1453.
 (63) Hernandez, S.; Ford, H.; Marquez, V. E. *Bioorg. Med. Chem.* **2002**, *10*, 2723–2730.
 (64) Seela, F.; Zulauf, M. *J. Chem. Soc., Perkin Trans. 1* **1999**, 479–488.
 (65) Peng, X.; Li, H.; Seela, F. *Nucleic Acids Res.* **2006**, *34*, 5987–6000.

- (66) Pangborn, A. B.; Giardello, M. A.; Grubbs, R. H.; Rosen, R. K.; Timmers, F. J. *Organometallics* **1996**, *15*, 1518–20.

4-Amino-3-(3'-*O*-*tert*-butyldimethylsilyloxypropyne)-1-(β -D-ribofuranosyl)-1*H*-pyrazolo[3,4-*d*]pyrimidine (10). To a solution of compound **9** (304 mg, 0.406 mmol) in anhydrous MeOH (10 mL) was added MeONa (25 mg, 0.45 mmol) until the pH reached 11.0. The mixture was stirred at room temperature for 1 h and neutralized with Amberlyst 15 ion-exchange resin. The resin was filtered and washed with MeOH, and the solvent was removed under vacuum. The residue was purified by flash silica gel column chromatography with CH₂Cl₂/CH₃OH (9:1 → 6:1) to give **10** as a white solid (124 mg, 70%). ¹H NMR (CD₃OD, 600 MHz): δ (ppm) 8.03 (s, 1H), 6.04 (d, *J* = 4.8 Hz, 1H), 4.53 (t, *J* = 4.8 Hz, 1H), 4.48 (s, 2H), 4.23 (t, *J* = 4.8 Hz, 1H), 3.92 (dd, *J* = 4.8, 8.4 Hz, 1H), 3.61 (dd, *J* = 3.6, 12.6 Hz, 1H), (dd, *J* = 5.4, 12.6 Hz, 1H), 0.76 (s, 9H), 0.01 (s, 6H). ¹³C NMR (CD₃OD, 150 MHz): δ (ppm) 166.3, 160.4, 157.8, 131.6, 105.6, 97.8, 94.3, 89.8, 79.6, 78.1, 75.3, 66.7, 55.7, 28.9, 21.8, -2.3. ESIHRMS: calcd for C₁₉H₃₀N₅O₅Si (M + H)⁺ 436.2016, obsd. 436.2027.

General Procedure for the Preparation of *N*-(Dimethylacetamide)-7-substituted-8-aza-7-deazaadenosine Analogues. *N,N*-Dimethylacetamide dimethyl acetal (3 equiv) was added to a solution of the ribonucleoside (0.25–1.02 mmol) in CH₃OH (1.3–8 mL), and the resulting reaction mixture was stirred at room temperature for 12 h. It was then concentrated and purified by flash column chromatography on a silica gel using 4% CH₃OH/CH₂Cl₂ followed by 6% CH₃OH/CH₂Cl₂.

4-[(Dimethylamino)ethylidene]amino-1-(β -D-ribofuranosyl)-1*H*-pyrazolo[3,4-*d*]pyrimidine (11). A white foam (45.4 mg, 54%). ¹H NMR (CD₃OD, 300 MHz): δ (ppm) 8.50 (s, 1H), 8.13 (s, 1H), 6.36 (d, *J* = 4.7 Hz, 1H), 4.87–4.83 (m, 1H), 4.53–4.5 (m, 1H), 4.19 (q, *J* = 4.4, 1H), 3.91–3.71 (m, 2H), 3.26 (s, 6H), 2.27 (s, 3H). ¹³C NMR (CD₃OD, 75 MHz): δ (ppm) 164.7, 164.2, 156.7, 155.7, 135.7, 110.1, 91.6, 87.1, 75.5, 72.8, 64.2, 39.1, 38.8, 17.6. HRFABMS: calcd for C₁₄H₂₁N₆O₄ (M + H)⁺ 337.1624, obsd 337.1631.

4-[(Dimethylamino)ethylidene]amino-3-bromo-1-(β -D-ribofuranosyl)-1*H*-pyrazolo[3,4-*d*]pyrimidine (12). (187 mg, 75%). ¹H NMR (CDCl₃, 600 MHz): δ (ppm) 8.27 (s, 1H), 6.23 (d, *J* = 6.0 Hz, 1H), 4.88 (dd, *J* = 5.4, 6.0 Hz, 1H), 4.46 (dd, *J* = 1.2, 5.4 Hz, 1H), 4.28 (d, *J* = 1.2 Hz, 1H), 3.90 (dd, *J* = 1.8, 12.6 Hz, 1H), 3.70 (dd, *J* = 1.2, 12.6 Hz, 1H), 3.28 (s, 3H), 3.16 (s, 3H), 2.12 (s, 3H). ¹³C NMR (CD₃OD, 150 MHz): δ (ppm) 162.6, 161.4, 156.6, 154.0, 122.2, 107.2, 92.2, 87.5, 74.8, 73.2, 63.8, 38.9, 17.6. ESIHRMS: calcd for C₁₄H₂₀BrN₆O₄ (M + H)⁺ 415.0729, obsd 415.0729.

4-[(Dimethylamino)ethylidene]amino-3-iodo-1-(β -D-ribofuranosyl)-1*H*-pyrazolo[3,4-*d*]pyrimidine (13). A yellow foam (305.3 mg, 65%). ¹H NMR (CD₃OD, 300 MHz): δ (ppm) 8.41 (s, 1H), 6.25 (d, *J* = 4.7 Hz, 1H), 4.78–4.75 (m, 1H), 4.44 (t, *J* = 4.7 Hz, 1H), 4.15–4.12 (m, 1H), 3.85–3.66 (m, 2H), 3.29 (s, 3H), 3.22 (s, 3H), 2.18 (s, 3H). ¹³C NMR (CD₃OD, 75 MHz): δ (ppm) 163.7, 157.0, 155.5, 111.8, 93.6, 91.3, 87.1, 75.4, 72.6, 64.1, 39.1, 18.0. HRESIFTMS: calcd for C₁₄H₂₀IN₆O₄ (M + H)⁺ 463.0591, obsd 463.0576.

4-[(Dimethylamino)ethylidene]amino-3-(3'-*O*-*tert*-butyldimethylsilyloxypropyne)-1-(β -D-ribofuranosyl)-1*H*-pyrazolo[3,4-*d*]pyrimidine (14). (167 mg, 86%). ¹H NMR (CDCl₃, 600 MHz): δ (ppm) 8.31 (s, 1H), 6.25 (d, *J* = 6.0 Hz, 1H), 5.93 (t, *J* = 5.4 Hz, 1H), 4.50 (s, 2H), 4.47 (dd, *J* = 1.2, 4.8 Hz, 1H), 4.29 (d, *J* = 1.8 Hz, 1H), 3.91 (dd, *J* = 1.8, 12.6 Hz, 1H), 3.71 (dd, *J* = 1.2, 12.6 Hz, 1H), 3.22 (s, 3H), 3.13 (s, 3H), 2.10 (s, 3H), 0.88 (s, 9H), 0.11 (s, 6H). ¹³C NMR (CDCl₃, 150 MHz): δ (ppm) 162.2, 161.9, 156.0, 153.3, 128.9, 109.0, 92.8, 91.9, 87.4, 76.4, 74.6, 72.8, 63.6, 52.1, 38.7, 25.8, 18.3, 17.5, -5.0, -5.1. ESIHRMS: calcd for C₂₃H₃₇N₆O₅Si (M + H)⁺ 505.2595, obsd 505.2588.

General Procedure for the Preparation of *N*-(Dimethylacetamide)-5'-*O*-(4,4'-dimethoxytrityl)-7-substituted-8-aza-7-deazaadenosine Analogues. Anhydrous pyridine (6.0 equiv), 4,4'-dimethoxytrityl chloride (1.1 equiv), and AgNO₃ (1.1 equiv) were consequently

added to a solution of a *N*-(dimethylacetamide)-protected derivative (1.08–3.96 mmol) in freshly distilled THF (5–15 mL). The resulting reaction mixture was stirred at room temperature for 12 h. It was then diluted with EtOAc (25 mL), filtered, and washed with saturated aqueous NaHCO₃ (1 × 40 mL). The organic portion was dried (Na₂SO₄), filtered, and concentrated under reduced pressure. Purification was carried out by flash column chromatography on a silica gel using CH₂Cl₂/CH₃OH/TEA 96:3:1.

4-[(Dimethylamino)ethylidene]amino-1-(β -D-ribofuranosyl)-5'-*O*-(4,4'-dimethoxytriphenylmethyl)-1*H*-pyrazolo[3,4-*d*]pyrimidine (15). A white foam (344.1 mg, 50%). ¹H NMR (CD₂Cl₂, 300 MHz): δ (ppm) 8.44 (s, 1H), 7.91 (s, 1H), 7.42–7.15 (m, 9H), 6.84–6.72 (m, 4H), 6.40 (d, *J* = 3.7 Hz, 1H), 4.93–4.91 (m, 1H), 4.6 (t, *J* = 5.13 Hz, 1H), 4.23–4.18 (m, 1H), 3.74 (s, 6H), 3.31–3.12 (m, 8H), 2.17 (s, 3H). ¹³C NMR (CD₂Cl₂, 75 MHz): δ (ppm) 163.1, 163.0, 159.0, 156.3, 155.5, 145.7, 136.6, 136.5, 134.6, 130.6, 128.7, 128.3, 128.2, 127.1, 113.6, 113.5, 109.3, 89.3, 86.5, 84.0, 74.3, 72.4, 64.9, 55.7, 39.0, 38.6, 30.2, 17.4. HRFABMS: calcd for C₃₅H₃₉N₆O₆ (M + H)⁺ 639.2931, obsd 639.2925.

4-[(Dimethylamino)ethylidene]amino-3-bromo-1-(β -D-ribofuranosyl)-5'-*O*-(4,4'-dimethoxytriphenylmethyl)-1*H*-pyrazolo[3,4-*d*]pyrimidine (16). A white foam (201 mg, 85%). ¹H NMR (CD₂Cl₂, 600 MHz): δ (ppm) 8.36 (s, 1H), 7.45–7.18 (m, 9H), 6.8–6.78 (m, 4H), 6.33 (d, *J* = 4.2 Hz, 1H), 4.90 (t, *J* = 4.8 Hz, 1H), 4.48 (t, *J* = 5.4 Hz, 1H), 4.20 (dd, *J* = 4.2, 8.4 Hz, 1H), 3.76 (s, 3H), 3.33 (dd, *J* = 4.2, 10.2 Hz, 1H), 3.24 (s, 3H), 3.20 (dd, *J* = 5.4, 10.2 Hz, 1H), 3.16 (s, 3H), 2.07 (s, 3H). ¹³C NMR (CD₂Cl₂, 150 MHz): δ (ppm) 158.7, 155.25, 145.3, 136.3, 136.2, 130.3, 128.4, 127.9, 126.8, 122.6, 113.2, 106.8, 88.7, 86.3, 83.9, 73.8, 72.0, 64.3, 55.4, 46.5, 38.9, 38.8, 17.7, 8.6. ESIHRMS: calcd for C₃₅H₃₈BrN₆O₆ (M + H)⁺ 717.2036, obsd 717.2048.

4-[(Dimethylamino)ethylidene]amino-3-iodo-1-(β -D-ribofuranosyl)-5'-*O*-(4,4'-dimethoxytriphenylmethyl)-1*H*-pyrazolo[3,4-*d*]pyrimidine (17). A white foam (352.8 mg, 70%). ¹H NMR (CD₂Cl₂, 300 MHz): δ (ppm) 8.34 (s, 1H), 7.48–7.16 (m, 9H), 6.8–6.77 (m, 4H), 6.40 (d, *J* = 4.9 Hz, 1H), 5.00 (t, *J* = 4.9, 1H), 4.46–4.43 (m, 1H), 4.26–4.23 (m, 1H), 3.74 (s, 6H), 3.38–3.02 (m, 8H), 2.14 (s, 3H). ¹³C NMR (CD₂Cl₂, 75 MHz): δ (ppm) 162.7, 162.2, 159.0, 156.3, 155.2, 145.6, 136.7, 136.5, 130.6, 128.7, 128.3, 127.1, 113.6, 110.7, 92.6, 88.8, 86.6, 84.5, 74.0, 72.4, 64.8, 55.7, 39.0, 17.8. HRESIFTMS: calcd for C₃₅H₃₈IN₆O₆ (M + H)⁺ 765.1897, obsd 765.1899.

4-[(Dimethylamino)ethylidene]amino-3-(3'-*O*-*tert*-butyldimethylsilyloxypropyne)-1-(β -D-ribofuranosyl)-5'-*O*-(4,4'-dimethoxytriphenylmethyl)-1*H*-pyrazolo[3,4-*d*]pyrimidine (18). A white foam (186 mg, 68%). ¹H NMR (CD₂Cl₂, 600 MHz): δ (ppm) 8.36 (s, 1H), 7.39–7.37 (m, 2H), 7.28–7.23 (m, 4H), 7.21–7.18 (m, 2H), 7.15–7.14 (m, 1H), 6.74–6.72 (m, 4H), 6.32 (d, *J* = 4.2 Hz, 1H), 4.88 (dd, *J* = 3.6, 4.8 Hz, 1H), 4.52 (s, 2H), 4.51 (t, *J* = 7.2 Hz, 1H), 4.15 (dd, *J* = 5.4, 9.6 Hz, 1H), 3.72 (s, 6H), 3.29 (dd, *J* = 4.2, 10.2 Hz, 1H), 3.19 (dd, *J* = 5.4, 10.2 Hz, 1H) 3.18 (brs, 3H), 3.11 (bs, 3H), 2.13 (s, 3H), 0.88 (s, 9H), 0.10 (s, 6H). ¹³C NMR (CD₂Cl₂, 150 MHz): δ (ppm) 168.0, 167.4, 164.0, 161.8, 160.3, 150.6, 141.6, 141.5, 135.6, 135.5, 134.7, 133.6, 133.3, 132.1, 118.5, 114.4, 97.0, 94.5, 91.6, 88.9, 82.5, 79.1, 77.4, 69.7, 60.7, 57.6, 51.8, 44.0, 31.1, 23.7, 22.6, 14.0, 0.0. ESIHRMS: calcd for C₄₄H₅₅N₆O₇Si (M + H)⁺ 807.3902, obsd 807.3886.

General Procedure for the Preparation of *N*-(Dimethylacetamide)-5'-*O*-(4,4'-dimethoxytrityl)-2'-*O*-(*tert*-butyldimethylsilyl)-7-substituted-8-aza-7-deazaadenosine Analogues. Triethylamine (1.9 equiv) and *tert*-butylchlorodimethylsilyl (1.1 equiv) were consequently added to a solution of 5'-*O*-DMT protected derivative (0.54–0.46 mmol) in freshly distilled THF (8 mL). AgNO₃ (1.1 equiv) was added after stirring for 5 min. The resulting reaction mixture was stirred at room temperature for 12 h. It was then diluted with EtOAc (25 mL), filtered, and washed with 5% aqueous NaHCO₃ (1 × 30 mL). The organic portion was dried (Na₂SO₄), filtered, and concentrated under reduced pressure. Purification was

carried out by flash column chromatography on a silica gel by using a solvent system listed for individual compounds. The identity of 2'-*O*-TBDMS isomer vs 3'-*O*-TBDMS isomer was confirmed by 2D-NMR (COSY).

4-[[Dimethylamino]ethylidene]amino-1-(β-D-ribofuranosyl)-5'-*O*-(4,4'-dimethoxytriphenylmethyl)-2'-*O*-(*tert*-butyldimethylsilyl)-1*H*-pyrazolo[3,4-*d*]pyrimidine (19). Chromatography, EtOAc/hexanes 1:2. 2'-*O*-TBDMS isomer, a white foam (155 mg, 38%). ¹H NMR (CD₂Cl₂, 300 MHz): δ (ppm) 8.53 (s, 1H), 7.99 (s, 1H), 7.49–7.42 (m, 9H), 6.78–6.76 (m, 4H), 6.35 (d, *J* = 4.9 Hz, 1H), 5.18 (t, *J* = 5.1 Hz, 1H), 4.35 (dd, *J* = 4.9 Hz, 1H), 4.17–4.13 (m, 1H), 3.76 (s, 6H), 3.78–3.11 (m, 8H), 2.74 (d, *J* = 4.9 Hz, 1H), 2.22 (s, 3H), 0.84 (s, 9H), 0.03 (s, 3H), –0.13 (s, 3H). ¹³C NMR (CD₂Cl₂, 75 MHz): δ (ppm) 163.4, 162.8, 159.0, 156.7, 156.2, 145.8, 136.8, 136.6, 134.7, 130.7, 128.8, 128.2, 127.1, 113.5, 109.5, 88.8, 86.6, 84.3, 75.2, 72.5, 64.7, 55.7, 39.0, 38.5, 26.0, 18.4, 17.3, –4.7, –4.9. HRFABMS: calcd for C₄₁H₅₃N₆O₆Si (M + H)⁺ 753.3796, obsd 753.3771.

4-[[Dimethylamino]ethylidene]amino-3-bromo-1-(β-D-ribofuranosyl)-5'-*O*-(4,4'-dimethoxytriphenylmethyl)-2'-*O*-(*tert*-butyldimethylsilyl)-1*H*-pyrazolo[3,4-*d*]pyrimidine (20). Chromatography, ethyl acetate/hexane 99:1. 2'-*O*-TBDMS, a white foam (135 mg, 55%). ¹H NMR (CD₂Cl₂, 600 MHz): δ (ppm) 8.62 (s, 1H), 7.62–7.52 (m, 2H), 7.51–7.48 (m, 4H), 7.38–7.36 (m, 2H), 7.31–7.28 (m, 1H), 6.93–6.90 (m, 4H), 6.42 (d, *J* = 5.4 Hz, 1H), 5.28 (t, *J* = 5.4, 1H), 4.36 (brs, 1H), 4.26 (dd, *J* = 3.6, 7.8 Hz, 1H), 3.87 (s, 6H), 3.49 (dd, *J* = 3.6, 10.8 Hz, 1H), 3.37 (s, 3H), 3.27 (s, 3H), 3.22 (dd, *J* = 4.2, 10.2 Hz, 1H), 2.82 (brs, 1H), 2.36 (s, 3H), 0.96 (s, 9H), 0.14 (s, 3H), –0.0 (s, 3H). ¹³C NMR (CD₂Cl₂, 150 MHz): δ (ppm) 167.6, 167.5, 163.8, 162.3, 161.6, 150.6, 141.6, 141.3, 135.5, 133.6, 133.1, 131.9, 127.5, 118.42, 118.41, 112.8, 93.3, 91.6, 89.3, 79.6, 77.3, 69.4, 60.5, 43.9, 43.6, 30.8, 23.2, 22.4, 0.2, 0.0. ESIHRMS: calcd for C₄₁H₅₂BrN₆O₆Si (M + H)⁺ 832.8777, obsd 832.8779.

4-[[Dimethylamino]ethylidene]amino-3-iodo-1-(β-D-ribofuranosyl)-5'-*O*-(4,4'-dimethoxytriphenylmethyl)-2'-*O*-(*tert*-butyldimethylsilyl)-1*H*-pyrazolo[3,4-*d*]pyrimidine (21). Chromatography, EtOAc. 2'-*O*-TBDMS, a white foam (123.5 mg, 30%). ¹H NMR (CD₂Cl₂, 300 MHz): δ (ppm) 8.53 (s, 1H), 7.55–7.18 (m, 9H), 6.85–6.82 (m, 4H), 6.33 (d, *J* = 5.6 Hz, 1H), 5.26 (t, *J* = 5.3 Hz, 1H), 4.27 (brs, 1H), 4.2 (dd, *J* = 3.2 Hz, 1H), 3.78 (s, 6H), 3.44–3.10 (m, 8H), 2.81 (brs, 1H), 2.26 (s, 3H), 0.85 (s, 9H), 0.05 (s, 3H), –0.1 (s, 3H). ¹³C NMR (CD₂Cl₂, 75 MHz): δ (ppm) 162.7, 162.6, 159.0, 157.0, 156.1, 145.7, 136.8, 136.5, 130.7, 128.8, 128.4, 127.1, 113.6, 111.1, 92.4, 88.5, 86.8, 84.5, 75.1, 72.6, 64.7, 55.7, 39.1, 38.9, 25.9, 18.4, 17.7, –4.6, –4.8. HRESIFTMS: calcd for C₄₁H₅₂IN₆O₆Si (M + H)⁺ 879.2762, obsd 879.2768.

4-[[Dimethylamino]ethylidene]amino-3-(3'-*O*-*tert*-butyldimethylsilyloxypropyne)-1-(β-D-ribofuranosyl)-5'-*O*-(4,4'-dimethoxytriphenylmethyl)-2'-*O*-(*tert*-butyldimethylsilyl)-1*H*-pyrazolo[3,4-*d*]pyrimidine (22). A white foam (83.3 mg, 52%). ¹H NMR (CD₂Cl₂, 600 MHz): δ (ppm) 8.65 (s, 1H), 7.62–7.60 (m, 2H), 7.50–7.46 (m, 4H), 7.40–7.36 (m, 2H), 7.32–7.29 (m, 1H), 6.93–6.90 (m, 4H), 6.45 (d, *J* = 4.8 Hz, 1H), 5.24 (t, *J* = 4.8 Hz, 1H), 4.68 (s, 2H), 4.41 (dd, *J* = 4.8, 9.6 Hz, 1H), 4.28 (dd, *J* = 3.6, 8.4 Hz, 1H), 3.89 (s, 6H), 3.49 (dd, *J* = 3.6, 10.2 Hz, 1H), 3.37 (brs, 3H), 3.31 (dd, *J* = 4.8, 10.2 Hz, 1H), 3.28 (brs, 3H), 2.82 (d, *J* = 5.4 Hz, 1H), 2.34 (s, 3H), 1.04 (s, 9H), 0.97 (s, 9H), 0.24 (s, 6H), 0.15 (s, 3H), 0.00 (s, 3H). ¹³C NMR (CD₂Cl₂, 150 MHz): δ (ppm) 168.3, 167.4, 164.0, 162.3, 162.2, 161.0, 150.7, 141.6, 141.5, 135.74, 135.71, 135.6, 134.7, 133.8, 133.7, 133.3, 132.1, 118.7, 118.6, 118.5, 114.7, 96.9, 93.92, 93.9, 91.7, 89.5, 89.4, 82.6, 80.1, 80.0, 77.5, 77.4, 69.6, 69.5, 60.7, 60.6, 57.8, 57.7, 57.6, 31.2, 31.1, 31.0, 30.9, 30.8, 23.7, 23.4, 22.5, 22.4, 0.4, 0.2, 0.14, 0.1, 0.05, 0.0. ESIHRMS: calcd for C₅₀H₆₉N₆O₇Si₂ (M + H)⁺ 921.4766, obsd 921.4765.

General Procedure for the Preparation of *N*-(Dimethylacetamide)-5'-*O*-(4,4'-dimethoxytrityl)-3'-*O*-[(2-cyanoethyl)(*N,N*-diisopropylamino)phosphino]-2'-*O*-(*tert*-butyldimethylsilyl)-7-substituted-8-aza-7-deazaadenosine Analogues. *N,N*-Diisopropylethylamine (6 equiv) and 2-cyanoethyl-(*N,N*-diisopropylamino)chlorophosphite (1.1 equiv) were consequently added to a solution of 5'-*O*-DMT, 2'-*O*-TBDMS protected derivative (0.18–0.11 mmol) in freshly distilled THF (1 mL). The resulting reaction mixture was stirred at room temperature for 12 h. It was then diluted with EtOAc (30 mL), filtered, and washed with 5% (w/v) aqueous NaHCO₃ (2 × 15 mL). The organic portion was dried (Na₂SO₄), filtered, and concentrated under reduced pressure. Purification was carried out by flash column chromatography on silica gel using the solvent system listed for individual compounds.

4-[[Dimethylamino]ethylidene]amino-1-(β-D-ribofuranosyl)-5'-*O*-(4,4'-dimethoxytriphenylmethyl)-3'-*O*-[(2-cyanoethyl)(*N,N*-diisopropylamino)phosphino]-2'-*O*-(*tert*-butyldimethylsilyl)-1*H*-pyrazolo[3,4-*d*]pyrimidine (23). Chromatography, EtOAc/hexanes/TEA 39:60:1. A white foam (137.9 mg, 78%). ³¹P NMR (CD₂Cl₂, 300 MHz): δ (ppm) 150.1, 148.5.

4-[[Dimethylamino]ethylidene]amino-3-bromo-1-(β-D-ribofuranosyl)-5'-*O*-(4,4'-dimethoxytriphenylmethyl)-3'-*O*-[(2-cyanoethyl)(*N,N*-diisopropylamino)phosphino]-2'-*O*-(*tert*-butyldimethylsilyl)-1*H*-pyrazolo[3,4-*d*]pyrimidine (24). Chromatography, ethyl acetate/TEA 99:1. A white foam (108 mg, 92%). ³¹P NMR (CD₂Cl₂, 300 MHz): δ (ppm) 151.5, 150.7, 149.8. ESIHRMS: calcd for C₅₀H₆₉BrN₈O₇PSi (M + H)⁺ 1031.3978, obsd 1031.3979.

4-[[Dimethylamino]ethylidene]amino-3-iodo-1-(β-D-ribofuranosyl)-5'-*O*-(4,4'-dimethoxytriphenylmethyl)-3'-*O*-[(2-cyanoethyl)(*N,N*-diisopropylamino)phosphino]-2'-*O*-(*tert*-butyldimethylsilyl)-1*H*-pyrazolo[3,4-*d*]pyrimidine (25). Chromatography, EtOAc/TEA 99:1. A white foam (110.9 mg, 96%). ³¹P NMR (CD₂Cl₂, 300 MHz): δ (ppm) 151.6, 149.7. HRESIFTMS: calcd for C₅₀H₆₉IN₈O₇PSi (M + H)⁺ 1079.3841, obsd 1079.3838.

4-[[Dimethylamino]ethylidene]amino-3-(3'-*O*-*tert*-butyldimethylsilyloxypropyne)-1-(β-D-ribofuranosyl)-5'-*O*-(4,4'-dimethoxytriphenylmethyl)-3'-*O*-[(2-cyanoethyl)(*N,N*-diisopropylamino)phosphino]-2'-*O*-(*tert*-butyldimethylsilyl)-1*H*-pyrazolo[3,4-*d*]pyrimidine (26). Purified by radial chromatography (1 mm plate), ethyl acetate/hexane/TEA 64:35:1. A white foam (92 mg, 91%). ³¹P NMR (CD₂Cl₂, 300 MHz): δ (ppm) 151.5, 149.9. ESIHRMS: calcd for C₅₉H₈₆N₈O₈PSi₂ (M + H)⁺ 1121.5845, obsd 1121.5840.

General Biochemical Procedures. Distilled, deionized water was used for all aqueous reactions and dilutions. Biochemical reagents were purchased from Sigma/Aldrich unless otherwise noted. Common enzymes were purchased from Roche, Promega, or New England Biolabs. Phosphoramidites **23–26** were synthesized as described above. [γ -³²P]ATP (6000 Ci/mmol) was obtained from Perkin-Elmer Life Sciences. Storage phosphor autoradiography was carried out using imaging plates from Eastman Kodak Co and a Molecular Dynamics Typhoon 9400 or Typhoon Trio.

Protein Overexpression and Purification. Human ADAR2 (WT) and ADAR2 (R455A) in yeast expression plasmid (YEPTOP2PGAL1) were overexpressed in *Saccharomyces cerevisiae* and purified as previously described.²⁶

Description of T375X, R455X Library Generation and Screening. A QuikChange XL site-directed mutagenesis kit (Stratagene) was used to generate plasmid libraries following the manufacturer's protocol. The two specified codons were randomized sequentially. Codon 375 was randomized first. To generate this library the following primers were used: 5'-GGTGATAAGT-GTTTCTACAGGANNNAATGTATTAATGGTGAATACA and 5'-TGTATTACCATTAAATACATTTNNTCTGTAGAAACACTTATCACC, where N represents an equal mixture of A, C, G, and T. The *S. cerevisiae* expression vector for human ADAR2 YEPTOP2PGAL1(T375Amber) was used as a PCR template.³⁰ This amber stop codon plasmid was used as a template to minimize the

over-representation of wild type DNA in the library. XL 10 gold *E. coli* cells were transformed with the resulting PCR products using ampicillin selection. Approximately 500 bacterial colonies were harvested, combined and grown in LB-ampicillin selection. Plasmid DNA was isolated using a QIAprep Spin Miniprep kit (Qiagen). This resulting library DNA was used as a template to randomize the 455 codon, where the following two primers were used: 5'-CCTCTCCCTGTGGAGATGCCNNNA TCT-TCTCACCATGAGCC and 5'-GGCTCATGTGGTGAGAA-GATNNGGCATCTCCACAGGGAGAGG. The PCR reaction was used to transform bacteria, and approximately 5000 colonies were picked to isolate the T375X, R455X DNA library. Randomization at the corresponding sites was confirmed by DNA sequencing.

Synthesis, Purification, and Mass Spectrometric Analysis of RNA. RNA oligonucleotides were synthesized on an ABI 394 synthesizer (DNA/Peptide Core Facility, University of Utah) using 5'-DMT, 2'-*O*-TBDMS protected β -cyanoethyl phosphoramidites on a 1.0 μ mol scale with coupling times of 25 min for more efficient coupling. Oligonucleotide deprotection and purification were carried out as previously described with the slight change for the deprotection of the 7-substituted-8-aza-7-deazaadenosine CPG-bound oligonucleotide.³² These RNA oligonucleotides were incubated with ammonium hydroxide at room temperature for 24 h prior to removal of TBDMS with neat triethylamine trihydrofluoride. The RNA oligonucleotides after polyacrylamide gel electrophoresis purification were submitted to mass spectrometric analysis at the Mass Spectrometry and Proteomics Core Facility, University of Utah. Oligonucleotides were analyzed in an acetonitrile solution at pH = 11 by electrospray ionization on a Quattro-II mass spectrometer (Micromass, Inc.). The solution was introduced at 3 μ L/min with ESI conditions of 2.7 kV capillary voltage, 35 eV cone voltage, and nitrogen nebulization. The instrument was scanned from 700 to 1400 *m/z*, and scans were combined for approximately 1 min. The multiply charged molecular ions were deconvoluted into a molecular mass spectrum using MaxEnt (Micromass, Inc.) software. The Quattro-II instrument was operated using Masslynx software version 3.4 (Micromass, Inc.). ESI mass spectrometry analysis of 26-mer RNA oligonucleotide containing compound **3**: calcd: 8455.1; obsd: 8456.1. ESI mass spectrometry analysis of RNA oligonucleotide containing compound **4**: calcd: 8535.06; obsd: 8534.0. ESI mass spectrometry analysis of RNA oligonucleotide containing compound **5**: calcd: 8582.1; obsd: 8581.8. ESI mass spectrometry analysis of RNA oligonucleotide containing compound **6**: calcd: 8510.18; obsd: 8510.1. To ensure the C7 substituent remains unaltered during the ADAR2 reaction, RNA containing 7-bromo-8-aza-7-deazaA was subjected to the deamination reaction, purified, and analyzed by mass spectrometry. ESI mass spectrometry analysis of RNA oligonucleotide containing compound **4**: calcd: 8535.06; obsd: 8534.0. Observed mass after deamination 8535.2.

Preparation of RNA Duplexes. The formation of labeled RNA duplexes with 8-aza-7-deazaA and 7-substituted-8-aza-7-deazaA modifications was carried out as previously described with the slight

change.³² A 10-fold excess of modified unlabeled strand was added, and the resulting mixture was hybridized to the unlabeled complement strand.

Deamination Assay. The deamination assay and data quantification were carried out as previously described with the slight change.³² Single turnover editing reactions are carried out with 250 nM ADAR2 or mutant ADAR2(R455A) and 25 nM labeled RNA duplexes.

Oligos were incubated in deamination buffer containing no enzyme for 90 min at 30 °C to determine if any degradation products arise that comigrate with the deamination product during TLC. No observable degradation products with similar RF values to those of the deaminated nucleotide analogue were observed.

Computational Methods. Hydration free energies (purine analogue + water \rightarrow C6-hydrated purine analogue) in water were calculated using the CPCMB3LYP/6-31+G(d,p) method.^{67–71} For calculations on the iodine-containing system, a split basis set was used: 6-31+G(d,p) was used for carbon, hydrogen, nitrogen, and oxygen, and the LANL2DZ basis set,⁷² with pseudopotential, was used for iodine. Geometries of all structures (purines with methyl groups in place of the sugar moiety, hydrated versions thereof, and water) were fully optimized in solvent, and UA0 radii⁷³ and a dielectric constant of 78.39 were used in all calculations. The GAUSSIAN program suite was used for all calculations.⁷⁴ Coordinates and energies can be found in the Supporting Information. Additional calculations using different methods and including different heterocycles will be reported separately.

Acknowledgment. P.A.B. acknowledges the National Institutes of Health for financial support in the form of Grant GM061115. We would like to acknowledge the assistance of mass spectrometry facilities at the University of Utah, the University of California, Davis, and the University of California, San Diego.

Supporting Information Available: NMR and mass spectra for new compounds, ESI mass spectra for modified oligoribonucleotides, deamination kinetic data, computed geometries and hydration free energies for 8-aza-7-deaza-purine analogues, and full ref 74. This material is available free of charge via the Internet at <http://pubs.acs.org>.

JA9034076

(67) Becke, A. D. *J. Chem. Phys.* **1993**, *98*, 5648–5652.

(68) Lee, C.; Yang, W.; Parr, R. G. *Phys. Rev. B: Solid State* **1988**, *37*, 785–789.

(69) Stephens, P. J.; Devlin, F. J.; Cabalowski, C. F.; Frisch, M. J. *J. Phys. Chem.* **1994**, *98*, 11623–11627.

(70) Barone, V.; Cossi, M. *J. Phys. Chem. A* **1998**, *102*, 1995–2001.

(71) Barone, V.; Cossi, M.; Tomasi, J. *J. Comput. Chem.* **1998**, *19*, 404–417.

(72) Hay, P. J.; Wadt, W. R. *J. Chem. Phys.* **1985**, *82*, 270–283.

(73) Takano, Y.; Houk, K. N. *J. Chem. Theory Comput.* **2005**, *1*, 70–77.

(74) Frisch, M. J.; et al. *Gaussian03*; Gaussian, Inc.